

Ultraslow Convergence to Ergodicity in Transient Subdiffusion

Tomoshige Miyaguchi^{1,*} and Takuma Akimoto²

¹*Department of Applied Physics, Osaka City University, Osaka 558-8585, Japan,*

²*Department of Mechanical Engineering, Keio University, Yokohama 223-8522, Japan*

(Dated: April 30, 2018)

We investigate continuous time random walks with truncated α -stable trapping times. We prove distributional ergodicity for a class of observables; namely, the time-averaged observables follow the probability density function called the Mittag–Leffler distribution. This distributional ergodic behavior persists for a long time, and thus the convergence to the ordinary ergodicity is considerably slower than in the case in which the trapping-time distribution is given by common distributions. We also find a crossover from the distributional ergodic behavior to the ordinary ergodic behavior.

PACS numbers: 05.40.Fb, 02.50.Ey, 87.15.Vv

The ergodic theorem ensures that time averages of observables converge to their ensemble averages as the averaging time tends to infinity. On the other hand, a distributional ergodic theorem states that the probability density functions (PDFs) of time averages converge to the Mittag–Leffler (ML) distribution. This property is called infinite ergodicity in dynamical system theory, because it is associated with infinite invariant measures [1]. Furthermore, in recent years, the distributional ergodic property has been found for some observables in stochastic models such as continuous time random walks (CTRWs) [2]. For example, the time-averaged mean square displacement (TAMSD) [Eq. (10)] for CTRWs is a random variable even in the long measurement time limit and its PDF follows the ML distribution. It has been pointed out that this distributional ergodic behavior is reminiscent of the observations in biological experiments that showed that TAMSDs of macromolecules are widely distributed depending on trajectories [3]. In addition to these biological systems, CTRW-type systems are used to explain a broad range of phenomena such as charge carrier transport in amorphous materials [4], tracer particle diffusion in an array of convection rolls [5], and human mobility [6].

One of the important problems on stochastic models such as CTRWs is to clarify the condition of the distributional ergodicity. It has already been known that a few observables including the TAMSD show the distributional ergodicity in CTRWs. But any general criterion for an observable to satisfy the distributional ergodicity is still unknown. Another important problem to elucidate is finite size effects [7]. For CTRW-type systems, a power law trapping-time distribution is usually assumed, and thus rare events—long-time trappings—characterize the long-time behavior. These rare events, however, are often limited by finite size effects. For example, if the random trappings are caused by an energetic effect in complex energy landscapes, the most stable state has the longest trapping time, thereby causing a cutoff in the trapping-

time distribution. In fact, for the case of macromolecules in cells, the origin of trappings is considered to be energetic disorder: strong bindings to the target site, weak bindings to non-specific sites, and intermediate bindings to sites that are similar to the target site [8]. Because the binding to the target site should be most stable with the longest trapping time, there must be a cutoff [8]. Similarly, if the trappings are due to an entropic effect such as diffusion in inner degrees of freedom (diffusion on comb-like structures is a simple example [9]; see also [10]), the finiteness of the phase space of inner degrees of freedom results in a cutoff. The CTRWs with such a trapping-time cutoff show distributional ergodic features for short-time measurements, and become ergodic in the ordinary sense for long-time measurements. But this transition from distributional ergodic regime to ordinary ergodic regime has not been elucidated.

In this study, we employ a truncated one-sided stable distribution [11] as the trapping-time distribution, and show that the distributional ergodic behavior persists for a remarkably long time compared to the case of common distributions with the same mean trapping time. We also show that the time-averaged quantities for a large class of observables exhibit the distributional ergodicity. As an example, numerical simulations for a diffusion coefficient are presented. We use the exponentially truncated stable distribution (ETSD) proposed in [12] and the numerical method presented in [13]. This ETSD is useful for rigorous analysis of transient behavior, because it is an infinitely divisible distribution [14] and thus its convoluted distribution or characteristic function can be explicitly derived [Eqs. (5) and (6)].

Truncated one-sided stable distribution.—In this study, we investigate CTRWs on d -dimensional hypercubic lattices. The lattice constant is set to unity, and for simplicity, the jumps are allowed only to the nearest-neighbor sites without preferences. Let $\mathbf{r}(t') \in \mathbb{Z}^d$ be the position of the particle at time t' . Moreover, we assume that the successive trapping times τ_k ($k = 1, 2, \dots$) between jumps are mutually independent and the trapping-time distribution is the ETSD $P_{\text{TL}}(\tau, \lambda)$ defined by the canonical

* tomo@a-phys.eng.osaka-cu.ac.jp

87 form of the infinitely divisible distribution [14]:

$$e^{\psi(\zeta, \lambda)} = \int_{-\infty}^{\infty} P_{\text{TL}}(\tau, \lambda) e^{i\zeta\tau} d\tau, \quad (1)$$

$$\psi(\zeta, \lambda) = \int_{-\infty}^{\infty} (e^{i\zeta\tau} - 1) f(\tau, \lambda) d\tau, \quad (2)$$

88 The function $f(\tau, \lambda)$ is defined by [12]

$$f(\tau, \lambda) = \begin{cases} 0, & (\tau < 0) \\ -c \frac{\tau^{-1-\alpha} e^{-\lambda\tau}}{\Gamma(-\alpha)}, & (\tau > 0), \end{cases} \quad (3)$$

89 where $\Gamma(x)$ is the gamma function, $c > 0$ is a scale factor,
90 and $\alpha \in (0, 1)$ is a constant. The parameter $\lambda \geq 0$ char-
91 acterizes the exponential cutoff [Eq. (6)]. When $\lambda = 0$,
92 $P_{\text{TL}}(\tau, \lambda)$ is the one-sided α -stable distribution with a
93 power law tail $P_{\text{TL}}(\tau, 0) \sim 1/\tau^{1+\alpha}$ as $\tau \rightarrow \infty$ [14]. The
94 function $\psi(\zeta, \lambda)$ can be expressed as follows:

$$\psi(\zeta, \lambda) = -c[(\lambda - i\zeta)^\alpha - \lambda^\alpha]. \quad (4)$$

95 Hence, we obtain $n\psi(\zeta, \lambda) = \psi(n^{1/\alpha}\zeta, n^{1/\alpha}\lambda)$, where $n \geq$
96 0 is an integer. Therefore, if τ_k ($k = 1, 2, \dots$) are mutually
97 independent random variables each following $P_{\text{TL}}(\tau_k, \lambda)$,
98 then the n -times convoluted PDF $P_{\text{TL}}^n(\tau, \lambda)$, i.e., the PDF
99 of the summation $T_n = \sum_{k=1}^n \tau_k$, is given by

$$P_{\text{TL}}^n(\tau, \lambda) = n^{-1/\alpha} P_{\text{TL}}(n^{-1/\alpha}\tau, n^{1/\alpha}\lambda). \quad (5)$$

100 This is an important outcome of the infinite divisibility
101 and makes it possible to analyze transient behavior of
102 CTRWs. Moreover, from Eq. (4) and the inverse trans-
103 form of Eq. (1), we obtain an explicit form of $P_{\text{TL}}(\tau, \lambda)$
104 through the similar calculation shown in [14]:

$$P_{\text{TL}}(\tau, \lambda) = -\frac{e^{c\lambda^\alpha - \lambda\tau}}{\pi\tau} \sum_{k=1}^{\infty} \frac{\Gamma(k\alpha + 1)}{k!} (-c\tau^{-\alpha})^k \sin(\pi k\alpha). \quad (6)$$

105 CTRWs with truncated α -stable trapping times.—Now,
106 we consider the time average of an observable $h(t')$: $\bar{h}_t \equiv$
107 $\int_0^t dt' h(t')/t$, where t is the total measurement time. We
108 assume that $h(t')$ can be expressed as

$$h(t') = \sum_{k=1}^{\infty} H_k \delta(t' - T_k), \quad (7)$$

109 where $T_k > 0$ ($k = 1, 2, \dots$) is the time when the k -th
110 jump occurs, and H_k ($k = 1, 2, \dots$) are random variables
111 satisfying $\langle H_k \rangle = \langle H \rangle$ and the ergodicity with respect to
112 the operational time k ,

$$\frac{1}{n} \sum_{k=1}^n H_k \simeq \langle H \rangle, \quad \text{as } n \rightarrow \infty. \quad (8)$$

113 To satisfy Eq. (8), the correlation function $\langle H_k H_{k+n} \rangle -$
114 $\langle H_k \rangle \langle H_{k+n} \rangle$ should decay more rapidly than $n^{-\gamma}$ with
115 some constant $\gamma > 0$ [9, 15]. It follows from Eqs. (7) and
116 (8) that

$$\bar{h}_t = \frac{1}{t} \sum_{k=1}^{N_t} H_k \simeq \frac{N_t}{t} \langle H \rangle, \quad (9)$$

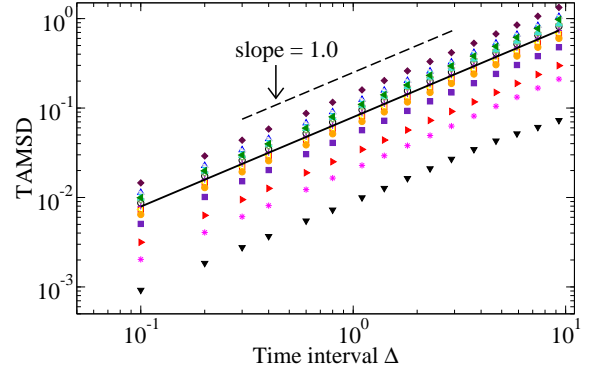


FIG. 1. (Color online) TAMSD $\overline{(\delta x)^2}(\Delta, t)$ vs time interval Δ (log-log plot) for the one-dimensional system ($d = 1$). Total measurement time t is set as $t = 10^5$ and other parameters as $\lambda = 10^{-5}$, $\alpha = 0.75$, and $c = 1$. The TAMSDs are calculated for 17 different realizations of trajectories; a different symbol corresponds to a different realization. The solid line is their ensemble average.

117 for long t , where N_t is the number of jumps until time t .
118 From this equation, we find that \bar{h}_t behaves similarly to
119 N_t . It is important that many time-averaged observables
120 for CTRWs can be defined by Eqs. (7) and (8). For
121 example, the TAMSD,

$$\overline{(\delta \mathbf{r})^2}(\Delta, t) \equiv \frac{1}{t - \Delta} \int_0^{t-\Delta} |\mathbf{r}(t' + \Delta) - \mathbf{r}(t')|^2 dt', \quad (10)$$

122 can be approximately obtained by the time average of
123 $h(t')$ with H_k defined as $H_k \equiv \Delta + 2 \sum_{l=1}^{k-1} (d\mathbf{r}_k \cdot d\mathbf{r}_l) \theta(\Delta -$
124 $(T_k - T_l))$, where d -dimensional vector $d\mathbf{r}_k$ is the displace-
125 ment at the time T_k , and $\theta(t)$ is defined by $\theta(t) = t$ for
126 $t \geq 0$, otherwise $\theta(t) = 0$. It is easy to see that $\langle H_k \rangle = \Delta$
127 and $\langle H_k H_{k+n} \rangle - \langle H_k \rangle \langle H_{k+n} \rangle = 0$ for $n \geq 1$. Using
128 Eq. (9), we have

$$\overline{(\delta \mathbf{r})^2}(\Delta, t) \simeq \Delta N_t / t. \quad (11)$$

129 From Eq. (11), we obtain a relation between N_t and the
130 diffusion coefficient of TAMSD as

$$D_t \simeq N_t / t. \quad (12)$$

131 In Fig.1, TAMSDs calculated from 17 different trajec-
132 tories are displayed as functions of time interval Δ . This
133 figure shows that the TAMSD grows linearly with Δ ,
134 and the diffusion coefficient D_t is distributed depending
135 on the trajectories.

137 PDF of time-averaged observables.—In this section, we
138 derive the PDF of time-averaged observables \bar{h}_t . Because
139 \bar{h}_t and N_t have the same PDF [Eq. (12)], we can study
140 N_t instead of \bar{h}_t . We have the following relations:

$$\begin{aligned} G(n; t) &\equiv \text{Prob}(N_t < n) = \text{Prob}(T_n > t) \\ &= \text{Prob}\left(\sum_{k=1}^n \tau_k > t\right), \end{aligned} \quad (13)$$

141 where $\text{Prob}(\cdot)$ is the probability and τ_k is the trapping
 142 time between $(k-1)$ -th and k -th jumps ($k = 1, 2, \dots$).
 143 From Eq. (13), we obtain

$$G(n; t) = \int_{n^{-1/\alpha t}}^{\infty} d\tau P_{\text{TL}}(\tau, n^{1/\alpha} \lambda), \quad (14)$$

144 where we have used Eq. (5) and the fact that τ_k ($k =$
 145 $1, 2, \dots$) are mutually independent. Furthermore, we
 146 change the variables from n to z as $n = t^\alpha z$ with t being
 147 set. Then, by using Eqs. (6), (13) and (14), we have

$$\text{Prob}\left(\frac{N_t}{t^\alpha} < z\right) = -\frac{e^{c(t\lambda)^\alpha z}}{\alpha\pi} \sum_{k=1}^{\infty} \frac{\Gamma(k\alpha + 1)}{k!k} \\ \times (-cz)^k \sin(\pi k\alpha) a_k(t), \quad (15)$$

148 where $a_k(t)$ ($k = 1, 2, \dots$) is defined by $a_k(t) \equiv$
 149 $\int_0^1 d\tau e^{-t\lambda\tau^{-1/(\alpha k)}}$. Differentiating Eq. (15) with respect
 150 to z , we have the PDF of $z = N_t/t^\alpha$:

$$f_\lambda(z; t) = -\frac{e^{c(t\lambda)^\alpha z}}{\alpha\pi} \sum_{k=1}^{\infty} \frac{\Gamma(k\alpha + 1)}{k!} (-c)^k \\ \times \left[\frac{c(t\lambda)^\alpha z}{k} + 1 \right] z^{k-1} \sin(\pi k\alpha) a_k(t). \quad (16)$$

151 Because of Eq. (9), Eq. (16) is the PDF of the time-
 152 averaged observables $\bar{h}_t t^{1-\alpha} / \langle H \rangle$ including the diffusion
 153 constant $D_t t^{1-\alpha}$ [Eq. (12)] as a special case. When $\lambda = 0$,
 154 the PDF $f_0(z)$, which is the ML distribution [1], is time-
 155 independent. Namely, the time-averaged observables are
 156 random variables even in the limit $t \rightarrow \infty$; this property
 157 is called the distributional ergodicity. On the other hand,
 158 when $\lambda > 0$, the PDF tends to a delta function. Thus, the
 159 time-averages converge to constant values as is expected
 160 from the ordinary ergodicity. The PDF of D_t is shown
 161 in Fig. 2 for three different measurement times t . It is
 162 clear that the PDF becomes narrower for a longer t . The
 163 analytical result given by Eq. (16) is also illustrated by
 164 the lines.

165 *Relative standard deviation.*—Next, in order to quan-
 166 tify a deviation from the ordinary ergodicity, we study a
 167 relative standard deviation (RSD) of time-averaged ob-
 168 servables $R(t) = \sqrt{\langle (\bar{h}_t)^2 \rangle_c} / \langle \bar{h}_t \rangle$, where $\langle \cdot \rangle$ is the ensem-
 169 ble average over trajectories and $\langle \cdot \rangle_c$ is the corresponding
 170 cumulant. If $R(t) \approx 0$, the system can be considered to
 171 be ergodic in the ordinary sense, whereas if $R(t) > 0$, the
 172 system is not ergodic. To derive an analytical expression
 173 for $R(t)$, we take the Laplace transform of Eq (14) with
 174 respect to t :

$$\tilde{G}(n; s) = \frac{1 - e^{-nc[(\lambda+s)^\alpha - \lambda^\alpha]}}{s}, \quad (17)$$

175 where we have defined $\tilde{G}(n; s)$ as $\tilde{G}(n; s) \equiv$
 176 $\int_0^\infty dt e^{-ts} G(n; t)$ and used Eq. (4). Next, we de-
 177 fine a function $g(n; s)$ by $g(n; s) := \tilde{G}(n+1; s) - \tilde{G}(n; s)$.

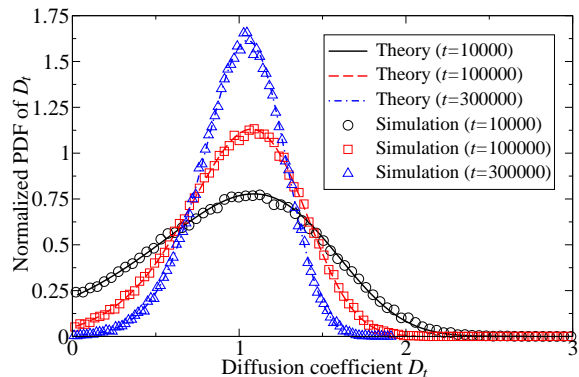


FIG. 2. (Color online) The PDF of the diffusion coefficient D_t for $d = 1$. Each PDF is normalized so that its mean value equals unity. D_t is calculated from TAMSD $\overline{(\delta x)^2}(\Delta, t)$ by least square fitting over the interval $0 < \Delta < 10$. The results for three different values of measurement times are presented: $t = 10^4$ (circles), 10^5 (squares), and 3×10^5 (triangles). The other parameters are set as $\lambda = 10^{-5}$, $\alpha = 0.75$, and $c = 1$. The lines correspond to the theoretical predictions given by Eq. (16). Note that no adjustable parameters were used to obtain these figures.

178 Then, by taking a (discrete) Laplace transform with
 179 respect to n , $\sum_{n=0}^{\infty} e^{-n\nu} g(n; s) \equiv \tilde{g}(\nu; s)$, we have

$$\tilde{g}(\nu; s) \simeq \frac{1}{s} \sum_{k=0}^{\infty} \left(-\frac{\nu}{c}\right)^k [(\lambda + s)^\alpha - \lambda^\alpha]^{-k}, \quad (18)$$

180 where we used an approximation by assuming $s, \lambda \ll 1$.
 181 From Eq. (18), we can derive arbitrary order of moments
 182 of N_t . For example, the first moment $\langle N_t \rangle$ is given by

$$\langle N_t \rangle \simeq \begin{cases} \frac{t^\alpha}{c\Gamma(\alpha + 1)}, & t \ll 1/\lambda \\ \frac{t}{c\lambda^{\alpha-1}\alpha} + \frac{1-\alpha}{2c\lambda^\alpha}, & t \gg 1/\lambda. \end{cases} \quad (19)$$

183 The ensemble-averaged mean square displacement
 184 (EAMSD) for CTRWs is known to be proportional to
 185 $\langle N_t \rangle$ [9]: $\langle (\delta r)^2 \rangle(t) \sim \langle N_t \rangle$. Thus, the EAMSD of the
 186 present model shows transient subdiffusion, i.e., subdif-
 187 fusion for short time scales and normal diffusion for long
 188 timescales [8]. Similarly, the second moment can be de-
 189 rived and we have the RSD for N_t as follows:

$$\frac{\sqrt{\langle N_t^2 \rangle_c}}{\langle N_t \rangle} \simeq \begin{cases} \sqrt{\frac{2\Gamma^2(\alpha+1)}{\Gamma(2\alpha+1)} - 1}, & t \ll 1/\lambda \\ (1-\alpha)^{1/2} \lambda^{-1/2} t^{-1/2}, & t \gg 1/\lambda. \end{cases} \quad (20)$$

190 Note that the RSDs for \bar{h}_t and D_t also follow the same
 191 relations, because they differ only in the scale factor
 192 [Eqs. (9) and (12)]. From these results, the crossover
 193 time t_c between the distributional and ordinary ergodic
 194 regimes is given by

$$t_c = \frac{(1-\alpha)}{2\Gamma^2(\alpha+1)/\Gamma(2\alpha+1) - 1} \lambda^{-1}. \quad (21)$$

195 As shown in Fig. 3, the RSD remains almost constant
 196 before the crossover time t_c , and starts to decay rapidly

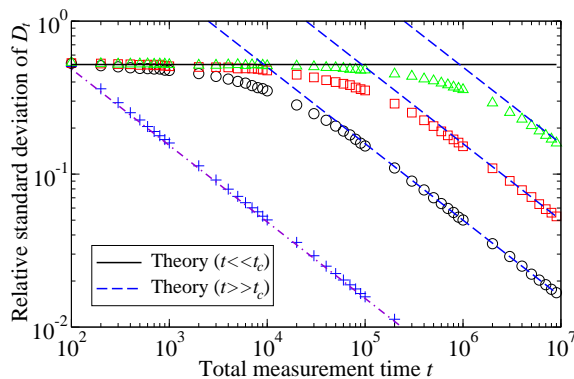


FIG. 3. (Color online) RSD $\sqrt{\langle D_t^2 \rangle_c} / \langle D_t \rangle$ vs total measurement time t for $d = 1$. D_t is calculated from the TAMSD $\overline{(\delta x)^2}(\Delta, t)$ by least square fitting over the interval $0 < \Delta < 1$. Three different values of λ are used: $\lambda = 10^{-4}$ (circles), 10^{-5} (squares), and 10^{-6} (triangles), and α and c are set as $\alpha = 0.75$ and $c = 1$, respectively. The lines correspond to the theoretical prediction given by Eq. (20); the solid line is the result for short time scales $t \ll t_c$, whereas the dashed lines are for long time scales $t \gg t_c$. The intersections of the solid and dashed lines correspond to the crossover times t_c given by Eq. (21). The pluses are the RSD for the case of the exponential distribution $P(\tau) = \exp(-\tau/\langle\tau\rangle)/\langle\tau\rangle$ with the same mean trapping time as the ETSD with $\lambda = 10^{-6}$ (triangles): $\langle\tau\rangle = c\lambda^{\alpha-1}\alpha$. The dot-dashed line is a theoretical prediction for the exponential distribution: $R(t) = (c\lambda^{\alpha-1}/t)^{1/2}$.

after the crossover. In Fig. 3, the RSD for the exponential trapping-time distribution which has the same mean trapping time $\langle\tau\rangle$ as the ETSD with $\lambda = 10^{-6}$ is also shown by pluses. It is clear that the RSD for exponential

distribution (pluses) decays much more rapidly than that for the ETSD (triangles).

Summary.—In this study, we have investigated the CTRWs with truncated α -stable trapping times. The three main results are as follows: (i) We proved the distributional ergodicity for short measurement times; namely, the time averages of observables behave as random variables following the ML distribution. Moreover, we derived the PDF at arbitrary measurement times. It is very interesting to compare this analytical formula [Eq. (16)] with the results for lipid granules reported recently [16]. We should also note that the limit distributions, the ML distribution for the case of observables studied in this paper, depends on the definition of observables [17]. (ii) We found that the distributional ergodic behavior persists for a long time. In other words, the convergence to the ordinary ergodicity is remarkably slow in contrast to the case in which the trapping-time distribution is given by common distributions such as the exponential distribution. This indicates that, in real experiments, the time-averaged quantities could behave as random variables even for considerably long measurement times. (iii) We found a crossover from the distributional ergodicity in the short-time regime to the ordinary ergodicity in the long-time regime. Finally, it is worth mentioning that these three main results are valid for a large class of observables. This implies that it is possible to choose an observable which is easy to measure experimentally. Then, the system parameters α and λ can be experimentally determined by the short- and long-time behavior of the RSD $R(t)$ [Eq. (20)], respectively.

-
- [1] J. Aaronson, *An Introduction to Infinite Ergodic Theory* (American Mathematical Society, Providence, 1997); T. Akimoto and T. Miyaguchi, Phys. Rev. E **82**, 030102 (2010).
- [2] Y. He, S. Burov, R. Metzler, and E. Barkai, Phys. Rev. Lett. **101**, 058101 (2008); A. Lubelski, I. M. Sokolov, and J. Klafter, *ibid.* **100**, 250602 (2008); T. Miyaguchi and T. Akimoto, Phys. Rev. E **83**, 031926 (2011).
- [3] I. Golding and E. C. Cox, Phys. Rev. Lett. **96**, 098102 (2006); I. Bronstein, Y. Israel, E. Kepten, S. Mai, Y. Shav-Tal, E. Barkai, and Y. Garini, *ibid.* **103**, 018102 (2009); Y. M. Wang, R. H. Austin, and E. C. Cox, *ibid.* **97**, 048302 (2006); A. Granéli, C. C. Yeykal, R. B. Robertson, and E. C. Greene, Proc. Natl. Acad. Sci. U.S.A **103**, 1221 (2006).
- [4] H. Scher and E. W. Montroll, Phys. Rev. B **12**, 2455 (1975).
- [5] W. Young, A. Pumir, and Y. Pomeau, Phys. Fluids A **1**, 462 (1989).
- [6] C. Song, T. Koren, P. Wang, and A. Barabasi, Nat Phys **6**, 818 (2010).
- [7] S. Burov, J. Jeon, R. Metzler, and E. Barkai, Physical Chemistry Chemical Physics **13**, 1800 (2011).
- [8] M. J. Saxton, Biophys. J. **92**, 1178 (2007).
- [9] J. Bouchaud and A. Georges, Phys. Rep. **195**, 127 (1990).
- [10] I. Goychuk and P. Hänggi, Proc. Natl. Acad. Sci. USA **99**, 3552 (2002).
- [11] R. N. Mantegna and H. E. Stanley, Phys. Rev. Lett. **73**, 2946 (1994).
- [12] I. Koponen, Phys. Rev. E **52**, 1197 (1995); H. Nakao, Phys. Lett. A **266**, 282 (2000).
- [13] J. Gajda and M. Magdziarz, Phys. Rev. E **82**, 011117 (2010).
- [14] W. Feller, *An Introduction to Probability Theory and its Applications*, 2nd ed., Vol. II (Wiley, New York, 1971) Chap. 17.
- [15] S. Burov, R. Metzler, and E. Barkai, Proc. Natl. Acad. Sci. U.S.A **107**, 13228 (2010).
- [16] J.-H. Jeon, V. Tejedor, S. Burov, E. Barkai, C. Selhuber-Unkel, K. Berg-Sørensen, L. Oddershede, and R. Metzler, Phys. Rev. Lett. **106**, 048103 (2011).
- [17] A. Rebenshtok and E. Barkai, Phys. Rev. Lett. **99**, 210601 (2007); J. Stat. Phys. **133**, 565 (2008); T. Akimoto, *ibid.* **132**, 171 (2008).